SCIENCE CHINA
Information Sciences

July 2024, Vol. 67, Iss. 7, 170302:1–170302:19
https://doi.org/10.1007/s11432-023-3968-9

• RESEARCH PAPER •

Special Topic: XAI-Enabled Network Automation for 5G and Beyond: Move Closer to Zero-Touch

Explainable-AI-based two-stage solution for WSN object localization using zero-touch mobile transceivers

Kai FANG[1], Junxin CHEN[2], Han ZHU[3], Thippa Reddy GADEKALLU[4], Xiaoping WU[5*] & Wei WANG[6*]

[1]*School of Mathematics and Computer Science, Zhejiang A&F University, Hangzhou* 311300*, China;*
[2]*School of Software, Dalian University of Technology, Dalian* 116081*, China;*
[3]*Faculty of Applied Sciences, Macao Polytechnic University, Macao* 999078*, China;*
[4]*Department of Electrical and Computer Engineering, Lebanese American University, Byblos* 1102 2801*, Lebanon;*
[5]*School of Information Engineering, Huzhou University, Huzhou* 313000*, China;*
[6]*Guangdong-Hong Kong-Macao Joint Laboratory for Emotional Intelligence and Pervasive Computing, Artificial Intelligence Research Institute, Shenzhen MSU-BIT University, Shenzhen* 518172*, China*

Received 2 August 2023/Revised 15 January 2024/Accepted 29 February 2024/Published online 28 June 2024

Abstract Artificial intelligence technology is widely used in the field of wireless sensor networks (WSN). Due to its inexplicability, the interference factors in the process of WSN object localization cannot be effectively eliminated. In this paper, an explainable-AI-based two-stage solution is proposed for WSN object localization. In this solution, mobile transceivers are used to enlarge the positioning range and eliminate the blind area for object localization. The motion parameters of transceivers are considered to be unavailable, and the localization problem is highly nonlinear with respect to the unknown parameters. To address this, an explainable AI model is proposed to solve the localization problem. Since the relationship among the variables is difficult to fully include in the first-stage traditional model, we develop a two-stage explainable AI solution for this localization problem. The two-stage solution is actually a comprehensive consideration of the relationship between variables. The solution can continue to use the constraints unused in the first-stage during the second-stage, thereby improving the performance of the solution. Therefore, the two-stage solution has stronger robustness compared to the closed-form solution. Experimental results show that the performance of both the two-stage solution and the traditional solution will be affected by numerical changes in unknown parameters. However, the two-stage solution performs better than the traditional solution, especially with a small number of mobile transceivers and sensors or in the presence of high noise. Furthermore, we have also verified the feasibility of the proposed explainable-AI-based two-stage solution.

Keywords explainable AI, object localization, semidefinite relaxation, mobile transceiver, two-stage solution, closed-form solution

1 Introduction

Localization is a fundamental problem for many applications, such as information monitoring in sensor networks and object tracking in radar or sonar systems [1–5]. When two signal sources are very close, some commonly used algorithms such as FOMP and 3D-FOMP can accurately detect them [6, 7]. As an important component for wireless signal radiation and reception, antennas play an important role in wireless communications. The antenna system consists of one or more antennas, which are responsible for converting electrical energy into electromagnetic waves and transmitting them into space, as well as receiving electromagnetic wave signals from space [8, 9]. The object lies in the region where a number of sensors are deployed. Through the signals emitted or reflected, the object position is uniquely determined by the sensors with known coordinations. The propagations of the signals result in all kinds of range-based measurements, including time of arrival (TOA) [10], time difference of arrival (TDOA) [11], angle of

* Corresponding author (email: wuxipu@gmail.com, ehomewang@ieee.org)

arrival (AOA) [12,13], and received signal strength (RSS) [14,15]. Among them, the TOA-based ranging measurement has become popular due to its low complexity and high efficiency.

From these range-based measurements, the object position is estimated by using various localization methods [16–19]. The direct search of the object position is subject to the high complexity [20, 21], and the traditional numerical solutions may be trapped in local convergence. Hence, recent literature focuses on the solution with the global optimum for the object position. The popular methods include the closed-form solutions [22, 23] and the convex relaxation techniques [24–27]. The closed-form solution represents the unknown parameter as an algebraic solution form by applying the weighted least squares (WLS) method [28–30]. Unfortunately, the constrained relationship among the variables is difficult to be exploited in the WLS solution. As a result, the performance of the WLS solution is poor, and the two-stage [31] and multi-stage WLS solutions [32] are proposed to improve the performance by availing of the constrained relationships. However, the performance of the closed-form solution is still poor due to its solution in multi-stages, especially at high noise levels.

Applying the convex relaxation process yields a semidefinite programming problem (SDP), the solution of which does not depend on any initialization from the users and always converges global optimum [33,34]. Hence, semidefinite relaxation (SDR) has been a popular method for its excellent performance in terms of localization accuracy. Different from the closed-form solutions, the constrained relationship can be directly included in the SDP problem. As a result, the SDP performs better than the closed-form solution due to its tight form. Recently, it has also been proven that the performance of the SDP solution is able to sufficiently approach the Cramér-Rao lower bound (CRLB) accuracy for certain localization problems [26,35,36], where the constrained relationships can be fully included by applying only one-stage SDR process. Unfortunately, it is also verified that the form is too relaxed for some SDP problems [25,37], where the object position is implicit in the constraints.

The minimum number of sensors needed for triangulation-based localization is two for the 2-D case or three for the 3-D case. The study of observability with respect to the sensor geometry configuration is a fundamental problem in localization systems [36]. Owing to the introduced auxiliary variables, the minimum number of sensors needed for the WLS solution is always greater than that of observability. Similar to the WLS solution, the performance of the SDP solution also highly depends on the sensor geometry, and the minimum number of sensors needed for the SDP solution needs to be investigated to ensure performance.

In this paper, we propose an explainable-AI-based two-stage solution for object localization using mobile transceivers, which bridges the sensors and the object [3, 38]. The signals emitted from the sensors, amplified and relayed by the transceivers, arrive at the object. After reflecting by the object, the signals are forwarded from the transceivers to the sensors. As a result, the observable range of the localization system is enlarged, and the system does not depend on the line of sight (LOS) propagation between the sensors and the object. Even if the object is blocked by obstacles, the mobile transceivers can also assist in detecting the object position accurately. Another application is the recently popular reconfigurable intelligent surface (RIS), which has been proposed to customize the radio environment for providing great benefits of localization [39, 40]. When the RISs are equipped with unmanned aerial vehicles (UAVs) [41] or autonomous underwater vehicles (AUVs), they can be dedicated to addressing the traditional positioning blind area problem caused by the signal block.

Recently, the localization problem using mobile transceivers is proposed in [42]. Mobile transceiver-based localization provides a scheme for object localization when the object lies in the blind area of positioning. In addition, the localization approach is very attractive since the motion parameters of the transceivers are considered to be unknown. The observability for this problem is provided in [42]. However, an efficient solution for this problem is not proposed. The localization problem using mobile transceivers is also rather challenging due to a large number of variables. By introducing auxiliary variables, we transform the nonlinear localization problem into a pseudo-linear form. However, the constrained relationships among the variables are difficult to include in the one-stage process. To handle the problem, we propose a two-stage solution for object localization using mobile transceivers. In addition, we also provide detailed proof of the feasibility of the two-stage by applying the rank analysis. The contributions of this work are summarized as follows.

(1) We propose an explainable-AI-based two-stage solution for object localization using mobile transceivers, and the relationships among the variables are included in the explainable AI model in two stages.

(2) We prove that the performance of the two-stage solution is capable of approaching optimal accuracy

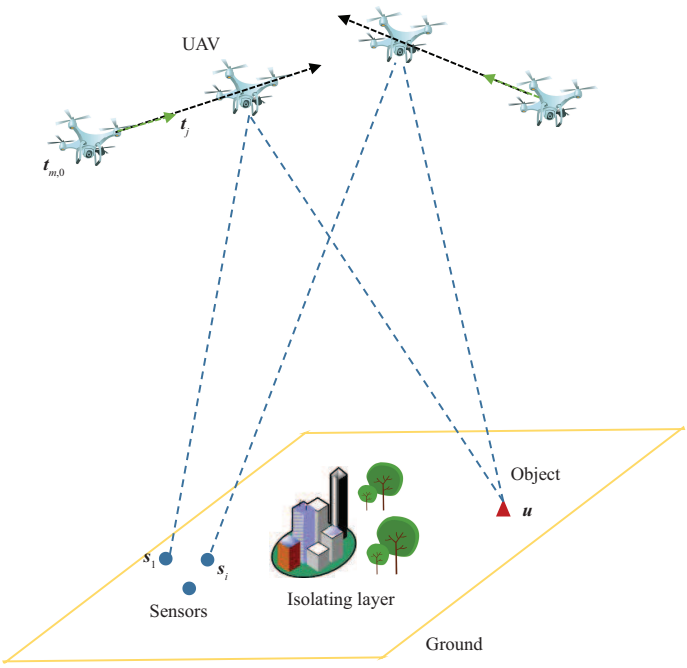

Figure 1 (Color online) Application scenario of object localization using transceivers.

at small noise levels.

(3) We provide the feasibility of the two-stage solution by applying the rank analysis and require at least $(M = 2, N = 3)$ for the 2-D case and $(M = 2, N = 4)$ for the 3-D case.

The rest of this paper is structured as follows. The problem formulation is described in Section 2. Section 3 presents the explainable-AI-based two-stage solution. The feasibility is given in Section 4. The performance analysis is provided in Section 5. The simulated results are evaluated in Section 6, and the conclusion is in Section 7.

Following the convention, bold lowercase letters and bold uppercase letters represent column vectors and matrices, respectively. The notations $(*)^{-1}$ and $(*)^{\mathrm{T}}$ represent matrix inverse and transpose operations. $\|*\|$ denotes ℓ_2 norm. $[\boldsymbol{a}]_i$ and $[\boldsymbol{a}]_{i:j}$ are the i-th element and the sub-vector containing the i-th to the j-th element of $\boldsymbol{a}$. $[\boldsymbol{A}]_{i,j}$ is the (i,j)-th element of matrix $\boldsymbol{A}$. $\boldsymbol{I}$ and $\boldsymbol{O}$ are identities and zero matrices, and $\boldsymbol{0}$ represents an all-zero vector. $\mathrm{tr}(\boldsymbol{A})$ and $\mathrm{rank}(\boldsymbol{A})$ stand for the trace and rank of $\boldsymbol{A}$, respectively. $\boldsymbol{A} \succeq \boldsymbol{0}$ indicates that $\boldsymbol{A}$ is positive semidefinite.

2 Problem formulation

Consider a q-dimensional space, in which the position $\boldsymbol{u}^o \in \mathbb{R}^q$ (q is 2 for 2-D or 3 for 3-D case) of an object requires to be determined. A localization system composed of N sensors is deployed to locate the object accurately. Each deployed sensor can both transmit and receive the signals, and the position of i-th sensor is known and defined as $\boldsymbol{s}_i$, $i = 1, 2, \ldots, N$. Besides, M transceivers are used to relay the signals from the sensors. These transceivers are attached to mobile equipment, such as UAVs or AUVs, and they are moving in constant velocity $\boldsymbol{v}_m^o$. As a result, the instant position of the m-th transceiver at the time step k can be modeled as

$$\boldsymbol{t}_j^o = \boldsymbol{t}_{m,0}^o + k\boldsymbol{v}_m^o, \tag{1}$$

where $\boldsymbol{t}_{m,0}^o$ is the starting position of the m-th transceiver, $j = (k-1)M + m$, $m = 1, 2, \ldots, M$, $k = 1, \ldots, K$.

Figure 1 shows a diagram of object localization using mobile transceivers. Both the sensors and the target are fixed. The propagation paths between the sensors and the target are blocked by obstacles and prevent direct communication. Hence, multiple mobile transceivers are introduced. The initial positions of the transceivers are placed in the near-field range of the sensors, and their function is to amplify and forward the signal. The transceivers can not only forward the incident waves from the sensors to the

object but also reverse the echo from the object to the sensors. Thus, the range measurements of the propagation paths are modeled as

$$d_p = \|\boldsymbol{s}_i - \boldsymbol{t}_j^o\| + \|\boldsymbol{u}^o - \boldsymbol{t}_j^o\| + \varepsilon_p, \tag{2}$$

where ε_p is additional noise, $p = (j-1)N + i$, $j = (k-1)M + m$, $m = 1, 2, \ldots, M$, $k = 1, \ldots, K$, $i = 1, \ldots, N$. For the signal reflected by the target or an obstacle in Figure 1, we can distinguish the main path and the interference path by analyzing the spectral characteristics of the signal. Next, by comparing the time of the sensor signal from transmission to reception, the propagation path of the signal can be determined.

To simplify the description, we define the vectors by

$$\boldsymbol{d} = [d_1, d_2, \ldots, d_{L_1}]^{\mathrm{T}},\ \boldsymbol{\varepsilon} = [\varepsilon_1, \varepsilon_2, \ldots, \varepsilon_{L_1}]^{\mathrm{T}}, \tag{3}$$

where $L_1 = KMN$. Without loss of generality, $\boldsymbol{\varepsilon}$ is assumed to obey a zero-mean Gaussian distribution with covariance matrix $\boldsymbol{\Sigma}$.

Let the starting positions of all the transceivers be a vector form $\boldsymbol{t}_0^o = [\boldsymbol{t}_{1,0}^{o\mathrm{T}}, \boldsymbol{t}_{2,0}^{o\mathrm{T}}, \ldots, \boldsymbol{t}_{M,0}^{o\mathrm{T}}]^{\mathrm{T}}$. Similarly, the velocities of all the transceivers are defined as a vector $\boldsymbol{v}^o = [\boldsymbol{v}_1^{o\mathrm{T}}, \boldsymbol{v}_2^{o\mathrm{T}}, \ldots, \boldsymbol{v}_M^{o\mathrm{T}}]^{\mathrm{T}}$. Using the measured $\boldsymbol{d}$, we aim at estimating the object position $\boldsymbol{u}^o$, even if the starting position $\boldsymbol{t}_0^o$ and the velocity $\boldsymbol{v}^o$ of the transceivers are unknown.

3 Two-stage solution

The range measurement is highly nonlinear with respect to the object position, and the numerical solution to this problem may be trapped in the local optimum. In this section, we propose the two-stage SDR solution that always converges to the global optimum. To conduct the SDR process, we first need to establish the pseudo-linear equation.

By moving $\|\boldsymbol{u}^o - \boldsymbol{t}_j^o\|$ to the left and squaring both sides, Eq. (2) becomes

$$\boldsymbol{s}_i^{\mathrm{T}}\boldsymbol{t}_j^o - d_p\alpha_j^o + 0.5\beta_j^o - 0.5(\boldsymbol{s}_i^{\mathrm{T}}\boldsymbol{s}_i^o - d_p^2) \simeq \|\boldsymbol{s}_i - \boldsymbol{t}_j^o\|\varepsilon_p, \tag{4}$$

where $\alpha_j^o = \|\boldsymbol{u}^o - \boldsymbol{t}_j^o\|$, $\beta_j^o = \alpha_j^{o2} - \boldsymbol{t}_j^{o\mathrm{T}}\boldsymbol{t}_j^o$.

Inserting (1) into (4) results in

$$\boldsymbol{s}_i^{\mathrm{T}}\boldsymbol{t}_{m,0}^o + k\boldsymbol{s}_i^{\mathrm{T}}\boldsymbol{v}_m^o - d_p\alpha_j^o + 0.5\beta_j^o - 0.5(\boldsymbol{s}_i^{\mathrm{T}}\boldsymbol{s}_i - d_p^2) \simeq \|\boldsymbol{s}_i - \boldsymbol{t}_j^o\|\varepsilon_p, \tag{5}$$

where $p = (j-1)N + i$, $j = (k-1)M + m$, $m = 1, 2, \ldots, M$, $k = 1, \ldots, K$, $i = 1, \ldots, N$.

Let us define an unknown vector $\boldsymbol{y}_1$ by

$$\boldsymbol{y}_1 = [\underbrace{\boldsymbol{t}_0^{o\mathrm{T}}}_{qM}, \underbrace{\boldsymbol{v}^{o\mathrm{T}}}_{qM}, \underbrace{\boldsymbol{\alpha}^{o\mathrm{T}}}_{KM}, \underbrace{\boldsymbol{\beta}^{o\mathrm{T}}}_{KM}]^{\mathrm{T}}, \tag{6}$$

where $\boldsymbol{\alpha}^o = [\alpha_1^o, \alpha_2^o, \ldots, \alpha_{KM}^o]^{\mathrm{T}}$, $\boldsymbol{\beta}^o = [\beta_1^o, \beta_2^o, \ldots, \beta_{KM}^o]^{\mathrm{T}}$, $\boldsymbol{y}_1 \in \mathbb{R}^{L_2}$, $L_2 = 2(q+K)M$.

As a result, the pseudo-linear equation in matrix form is expressed as

$$\boldsymbol{G}_1\boldsymbol{y}_1 - \boldsymbol{h}_1 = \boldsymbol{B}_1\boldsymbol{\varepsilon}. \tag{7}$$

According to (5), $\boldsymbol{G}_1$, $\boldsymbol{h}_1$, and $\boldsymbol{B}_1$ are defined as

$$\begin{aligned}
&[\boldsymbol{G}_1]_{p,q(m-1)+(1:q)} = \boldsymbol{s}_i^{\mathrm{T}}, \quad && [\boldsymbol{G}_1]_{p,q(m+M-1)+(1:q)} = k\boldsymbol{s}_i^{\mathrm{T}},\\
&[\boldsymbol{G}_1]_{p,2qM+j} = -d_p, && [\boldsymbol{G}_1]_{p,(2q+K)M+j} = 0.5,\\
&[\boldsymbol{h}_1]_p = 0.5(\boldsymbol{s}_i^{\mathrm{T}}\boldsymbol{s}_i - d_p^2), && [\boldsymbol{B}_1]_{p,p} = \|\boldsymbol{s}_i - \boldsymbol{t}_j^o\| \simeq \|\boldsymbol{s}_i - \boldsymbol{t}_j\|,
\end{aligned} \tag{8}$$

where $\boldsymbol{t}_j$ is the estimate of $\boldsymbol{t}_j^o$.

From the definitions of α_i^o and β_i^o, the variables defined in $\boldsymbol{y}_1$ have the following constrained relationships:

$$[\boldsymbol{y}_1]_{2qM+j} = \|\boldsymbol{u}^o - [\boldsymbol{y}_1]_{m_1+(1:q)} - k[\boldsymbol{y}_1]_{m_2+(1:q)}\|, \tag{9a}$$

$$- [\boldsymbol{y}]^{\mathrm{T}}_{m_1+(1:q)}[\boldsymbol{y}]_{m_1+(1:q)} - 2k[\boldsymbol{y}]^{\mathrm{T}}_{m_1+(1:q)}[\boldsymbol{y}]_{m_2+(1:q)} - k^2[\boldsymbol{y}]^{\mathrm{T}}_{m_2+(1:q)}[\boldsymbol{y}]_{m_2+(1:q)} + [\boldsymbol{y}]^2_{M_1+j} = [\boldsymbol{y}]_{M_2+j}, \tag{9b}$$

where $m_1 = q(m-1)$, $m_2 = q(m+M-1)$, $M_1 = 2qM$, $M_2 = 2qM + KM$, $j = (k-1)M + m$, $m = 1, 2, \ldots, M$, $k = 1, \ldots, K$.

According to the established pseudo-linear equation of (7), the constrained weighted least squares (CWLS) problem of the object position estimation can be formulated as

$$\begin{aligned} \min_{\boldsymbol{y}_1, \boldsymbol{u}^o} \quad & (\boldsymbol{G}_1\boldsymbol{y}_1 - \boldsymbol{h}_1)^{\mathrm{T}}\boldsymbol{W}_1(\boldsymbol{G}_1\boldsymbol{y}_1 - \boldsymbol{h}_1) \\ \text{s.t.} \quad & \text{(9a), (9b)}, \end{aligned} \tag{10}$$

where the weighting matrix $\boldsymbol{W}_1$ is approximately equal to the inverse of the covariance matrix with respect to the noise term $\boldsymbol{B}_1\boldsymbol{\varepsilon}$, and

$$\boldsymbol{W}_1 \simeq (\boldsymbol{B}_1\boldsymbol{\Sigma}\boldsymbol{B}_1^{\mathrm{T}})^{-1}. \tag{11}$$

The CWLS problem (10) has two constraints (9a) and (9b). Note that the object position $\boldsymbol{u}^o$ is implicit in the constraint (9a) and not defined in $\boldsymbol{y}_1$. Accordingly, we first consider the CWLS problem that does not include the constraint (9a) in the stage-one SDR process. As a result, the CWLS problem (10) is reduced to

$$\begin{aligned} \min_{\boldsymbol{y}_1} \quad & (\boldsymbol{G}_1\boldsymbol{y}_1 - \boldsymbol{h}_1)^{\mathrm{T}}\boldsymbol{W}_1(\boldsymbol{G}_1\boldsymbol{y}_1 - \boldsymbol{h}_1) \\ \text{s.t.} \quad & \text{(9b)}. \end{aligned} \tag{12}$$

3.1 Stage-one solution

To conduct the SDR process, we define an unknown matrix by

$$\boldsymbol{Y}_1 = \begin{bmatrix} \boldsymbol{y}_1\boldsymbol{y}_1^{\mathrm{T}} & \boldsymbol{y}_1 \\ \boldsymbol{y}_1^{\mathrm{T}} & 1 \end{bmatrix}. \tag{13}$$

Obviously, the defined $\boldsymbol{Y}_1$ satisfies

$$\boldsymbol{Y}_1 \succeq \boldsymbol{0},\ [\boldsymbol{Y}_1]_{L_3,L_3} = 1, \tag{14a}$$

$$\mathrm{rank}(\boldsymbol{Y}_1) = 1, \tag{14b}$$

where $L_3 = 2(q+K)M + 1$. When $\boldsymbol{Y}_1$ is defined, the cost function in (12) is also rewritten as

$$(\boldsymbol{G}_1\boldsymbol{y}_1 - \boldsymbol{h}_1)^{\mathrm{T}}\boldsymbol{W}_1(\boldsymbol{G}_1\boldsymbol{y}_1 - \boldsymbol{h}_1) = \mathrm{tr}(\boldsymbol{C}_1\boldsymbol{Y}_1), \tag{15}$$

where

$$\boldsymbol{C}_1 = \begin{bmatrix} \boldsymbol{G}_1^{\mathrm{T}}\boldsymbol{W}_1\boldsymbol{G}_1 & -\boldsymbol{G}_1^{\mathrm{T}}\boldsymbol{W}_1\boldsymbol{h}_1 \\ -\boldsymbol{h}_1^{\mathrm{T}}\boldsymbol{W}_1\boldsymbol{G}_1 & \boldsymbol{h}_1^{\mathrm{T}}\boldsymbol{W}_1\boldsymbol{h}_1 \end{bmatrix}. \tag{16}$$

Besides, Eq. (9b) becomes

$$\begin{aligned} [\boldsymbol{Y}_1]_{M_1+j,M_1+j} = {} & \mathrm{tr}(k^2[\boldsymbol{Y}_1]_{m_2+(1:q),m_2+(1:q)}) + [\boldsymbol{Y}_1]_{M_2+j,L_3} \\ & + \mathrm{tr}([\boldsymbol{Y}_1]_{m_1+(1:q),m_1+(1:q)} + 2k[\boldsymbol{Y}_1]_{m_1+(1:q),m_2+(1:q)}), \end{aligned} \tag{17}$$

where $L_3 = 2(q+K)M + 1$, and the definitions of j, m_1, m_2, M_1, and M_2 are the same as those of (9b). As a result, the CWLS problem (12) is equivalent to representing as

$$\begin{aligned} \min_{\boldsymbol{Y}_1} \quad & \mathrm{tr}(\boldsymbol{C}_1\boldsymbol{Y}_1) \\ \text{s.t.} \quad & \text{(14a), (14b), (17)}. \end{aligned} \tag{18}$$

Problem (18) is still non-convex due to the rank-one constraint (14b). Fortunately, dropping the rank-one constraint (14b) yields the stage-one SDR problem:

$$\begin{aligned} \min_{\boldsymbol{Y}_1} \quad & \mathrm{tr}(\boldsymbol{C}_1\boldsymbol{Y}_1) \\ \text{s.t.} \quad & \text{(14a), (17).} \end{aligned} \tag{19}$$

The SDR problem (19) can be effectively solved using a convex optimization package such as SEDUMI and SDPT3. Extracting from the estimated $\boldsymbol{Y}_1$, we can obtain the estimate of $\boldsymbol{y}_1$ by

$$\boldsymbol{y}_1 = [\boldsymbol{Y}_1]_{1:L_2,L_3}. \tag{20}$$

The solution $\boldsymbol{W}_1$ requires $\boldsymbol{B}_1$ that depends on the value of $\boldsymbol{t}_j^o$. Unfortunately, the true $\boldsymbol{x}_j^o$ is unknown from (8). Initially, setting $\boldsymbol{W}_1$ to an identity yields a coarse estimate of $\boldsymbol{t}_j^o$ since the solution is insensitive to the weighting matrix $\boldsymbol{W}_1$. Using the coarse estimate form $\boldsymbol{W}_1$ will give a better solution.

The CWLS problem (12) is equivalent to representing the problem (18), which is further relaxed as the stage-one SDR problem (19) by dropping the rank-one constraint (14b). It seems that the stage-one SDR problem is a relaxed form of the CWLS problem (12). In practice, the stage-one SDR problem (19) is tight enough. In [35,43], it is proven that the SDR solution is rank-one over the small noise region when $\boldsymbol{G}_1$ is full column rank. As a result, the performance of the stage-one SDR solution is also equivalent to that of the CWLS problem (12). Hence, we derive the estimation error of $\boldsymbol{y}_1$ from the CWLS problem (12). Let us define a vector $\boldsymbol{\phi} = [\boldsymbol{y}_1]_{1:2qM+KM}$, and $\Delta\boldsymbol{\phi}$ is the estimation error of $\boldsymbol{\phi}$. In the CWLS problem (12), the variable $\boldsymbol{\beta}$ is determined by $\boldsymbol{\phi}$, and both of them are included in $\boldsymbol{y}_1$. Hence, $\Delta\boldsymbol{\phi}$ is given by

$$\frac{\partial(\boldsymbol{G}_1\boldsymbol{y}_1)}{\partial\boldsymbol{y}_1^{\mathrm{T}}}\frac{\partial\boldsymbol{y}_1}{\partial\boldsymbol{\phi}^{\mathrm{T}}}\Delta\boldsymbol{\phi} \simeq \boldsymbol{B}_1\boldsymbol{\varepsilon}. \tag{21}$$

Let us define

$$\boldsymbol{H}_1 = \frac{\partial\boldsymbol{y}_1}{\partial\boldsymbol{\phi}^{\mathrm{T}}}. \tag{22}$$

Applying the definition of $\boldsymbol{y}_1$, we have

$$\begin{aligned} &[\boldsymbol{H}_1]_{1:M_2,1:M_2} = \boldsymbol{I}, && [\boldsymbol{H}_1]_{M_2+j,m_1+(1:q)} = -2\boldsymbol{t}_j^{o\mathrm{T}}, \\ &[\boldsymbol{H}_1]_{M_2+j,m_2+(1:q)} = -2k\boldsymbol{t}_j^{o\mathrm{T}}, && [\boldsymbol{H}_1]_{M_2+j,M_1+j} = 2\alpha_j^o, \end{aligned} \tag{23}$$

where the definitions of j, m_1, m_2, M_1, and M_2 are also the same as those of (9b), $\boldsymbol{t}_j^o$ and α_j^o can be approximated by the estimates.

As a result, the WLS solution to (21) gives

$$\Delta\boldsymbol{\phi} = (\boldsymbol{A}_1^{\mathrm{T}}\boldsymbol{W}_1\boldsymbol{A}_1)^{-1}\boldsymbol{A}_1^{\mathrm{T}}\boldsymbol{W}_1\boldsymbol{B}_1\boldsymbol{\varepsilon}, \tag{24}$$

where $\boldsymbol{A}_1 = \boldsymbol{G}_1\boldsymbol{H}_1$. At the low noise levels, the noise in $\boldsymbol{A}_1$ can be insignificant. Thus, the covariance of $\Delta\boldsymbol{\phi}$ is

$$\mathrm{cov}(\Delta\boldsymbol{\phi}) = (\boldsymbol{A}_1^{\mathrm{T}}\boldsymbol{W}_1\boldsymbol{A}_1)^{-1}. \tag{25}$$

3.2 Stage-two solution

The stage-one SDR is derived from the CWLS problem (12) that does not consider the constraint (9a). In the stage-two SDR, we solve the object position by availing of the constraint (9a). The estimation error gives

$$\boldsymbol{t}_{m,0}^o - \boldsymbol{t}_{m,0} = -\Delta\boldsymbol{t}_{m,0}, \tag{26a}$$

$$\boldsymbol{v}_m^o - \boldsymbol{v}_m = -\Delta\boldsymbol{v}_m,\ m = 1,2,\ldots,M. \tag{26b}$$

Squaring both sides of $\alpha_j^o = \|\boldsymbol{u}^o - \boldsymbol{t}_j^o\|$, and applying the definition of $\boldsymbol{\phi}^o$ and $\boldsymbol{\phi}^o = \boldsymbol{\phi} - \Delta\boldsymbol{\phi}$ yield

$$\boldsymbol{t}_j^{\mathrm{T}}\boldsymbol{u}^o - 0.5\boldsymbol{u}^{o\mathrm{T}}\boldsymbol{u}^o - 0.5\boldsymbol{t}_j^{\mathrm{T}}\boldsymbol{t}_{m,0}^o - 0.5k\boldsymbol{t}_j^{\mathrm{T}}\boldsymbol{v}_m^o + [\boldsymbol{\phi}]_{2qM+j}^2 \simeq (\boldsymbol{u}^o - 0.5\boldsymbol{t}_j^o)^{\mathrm{T}}\Delta\boldsymbol{t}_j + [\boldsymbol{\phi}]_{2qM+j}[\Delta\boldsymbol{\phi}]_{2qM+j}, \tag{27}$$

where $\boldsymbol{t}_j = [\boldsymbol{\phi}]_{m_1+(1:q)} + k[\boldsymbol{\phi}]_{m_2+(1:q)}$.

Let the unknown vector be

$$\boldsymbol{y}_2 = [\boldsymbol{u}^{o\mathrm{T}}, \boldsymbol{t}_0^{o\mathrm{T}}, \boldsymbol{v}^{o\mathrm{T}}, \boldsymbol{u}^{o\mathrm{T}}\boldsymbol{u}^{o}]^{\mathrm{T}} \in \mathbb{R}^{L_4}, \tag{28}$$

where $L_4 = q + 2qM + 1$. From (26a), (26b), and (27), the pseudo-linear equation in matrix form is

$$\boldsymbol{G}_2\boldsymbol{y}_2 - \boldsymbol{h}_2 = \boldsymbol{B}_2\Delta\boldsymbol{\phi}. \tag{29}$$

The detailed definitions of $\boldsymbol{G}_2$, $\boldsymbol{h}_2$, and $\boldsymbol{B}_2$ are provided in Appendix A.

From (29), the CWLS problem is formulated as

$$\begin{aligned} \min_{\boldsymbol{y}_2} \quad & (\boldsymbol{G}_2\boldsymbol{y}_2 - \boldsymbol{h}_2)^{\mathrm{T}}\boldsymbol{W}_2(\boldsymbol{G}_2\boldsymbol{y}_2 - \boldsymbol{h}_2) \\ \text{s.t.} \quad & [\boldsymbol{y}_2]_{L_4} = [\boldsymbol{y}_2]_{1:q}^{\mathrm{T}}[\boldsymbol{y}_2]_{1:q}, \end{aligned} \tag{30}$$

where the weighting matrix $\boldsymbol{W}_2$ is approximated by

$$\boldsymbol{W}_2 \simeq (\boldsymbol{B}_2\mathrm{cov}(\Delta\boldsymbol{\phi})\boldsymbol{B}_2^{\mathrm{T}})^{-1}. \tag{31}$$

To convert problem (30) into a convex SDP form, we define a matrix by

$$\boldsymbol{Y}_2 = \begin{bmatrix} \boldsymbol{y}_2\boldsymbol{y}_2^{\mathrm{T}} & \boldsymbol{y}_2 \\ \boldsymbol{y}_2^{\mathrm{T}} & 1 \end{bmatrix}. \tag{32}$$

$\boldsymbol{Y}_2$ needs to satisfy

$$\boldsymbol{Y}_2 \succeq \boldsymbol{0},\ [\boldsymbol{Y}_2]_{L_5,L_5} = 1, \tag{33a}$$

$$\mathrm{rank}(\boldsymbol{Y}_2) = 1, \tag{33b}$$

where $L_5 = q + 2qM + 2$. When $\boldsymbol{Y}_2$ is defined, the constraint in problem (30) becomes

$$[\boldsymbol{Y}_2]_{L_4,L_5} = \mathrm{tr}([\boldsymbol{Y}_2]_{1:q,1:q}). \tag{34}$$

Similar to the procedure of (18) and (19), the CWLS problem (30) can be relaxed as the stage-two SDR problem:

$$\begin{aligned} \min_{\boldsymbol{Y}_2} \quad & \mathrm{tr}(\boldsymbol{C}_2\boldsymbol{Y}_2) \\ \text{s.t.} \quad & \text{(33a), (34)}, \end{aligned} \tag{35}$$

where

$$\boldsymbol{C}_2 = \begin{bmatrix} \boldsymbol{G}_2^{\mathrm{T}}\boldsymbol{W}_2\boldsymbol{G}_2 & -\boldsymbol{G}_2^{\mathrm{T}}\boldsymbol{W}_2\boldsymbol{h}_2 \\ -\boldsymbol{h}_2^{\mathrm{T}}\boldsymbol{W}_2\boldsymbol{G}_2 & \boldsymbol{h}_2^{\mathrm{T}}\boldsymbol{W}_2\boldsymbol{h}_2 \end{bmatrix}. \tag{36}$$

Solving the stage-two SDR problem yields the estimates of $\boldsymbol{u}$, $\boldsymbol{t}_0$, and $\boldsymbol{v}$ which are given by

$$\boldsymbol{u} = [\boldsymbol{Y}]_{1:q,L_5},\ \boldsymbol{t}_0 = [\boldsymbol{Y}]_{q+(1:qM),L_5},\ \boldsymbol{v} = [\boldsymbol{Y}]_{q+qM+(1:qM),L_5}. \tag{37}$$

The independent variable in the CWLS problem (30) is $\boldsymbol{\varphi}^o = [\boldsymbol{u}^{o\mathrm{T}}, \boldsymbol{t}_0^{o\mathrm{T}}, \boldsymbol{v}^{o\mathrm{T}}]^{\mathrm{T}}$. The estimated value of $\boldsymbol{\varphi}^o$ is defined as $\boldsymbol{\varphi}$, and $\Delta\boldsymbol{\varphi}$ is its estimation error. Similar to the procedure of (21)–(25), we can obtain the covariance of estimation error $\Delta\boldsymbol{\varphi}$,

$$\mathrm{cov}(\Delta\boldsymbol{\varphi}) = (\boldsymbol{A}_2^{\mathrm{T}}\boldsymbol{W}_2\boldsymbol{A}_2)^{-1}, \tag{38}$$

where $\boldsymbol{A}_2 = \boldsymbol{G}_2\boldsymbol{H}_2$,

$$\boldsymbol{H}_2 = \frac{\partial\boldsymbol{y}_2}{\partial\boldsymbol{u}^{o\mathrm{T}}}. \tag{39}$$

The definition of $\boldsymbol{y}_2$ gives

$$[\boldsymbol{H}_2]_{1:q+2qM,1:q+2qM} = \boldsymbol{I},\ [\boldsymbol{H}_2]_{q+2qM+1,1:q} = 2\boldsymbol{u}^{o\mathrm{T}} \simeq 2\boldsymbol{u}^{\mathrm{T}}. \tag{40}$$

The solution of $\boldsymbol{W}_2$ requires $\boldsymbol{B}_2$ that depends on the value of $\boldsymbol{u}^o$. Unfortunately, $\boldsymbol{u}^o$ is unavailable at the beginning. Initially, setting $\boldsymbol{W}_2$ to an identity gives a coarse estimate of $\boldsymbol{u}^o$, which is used to form $\boldsymbol{B}_2$ and $\boldsymbol{W}_2$. The newly formed $\boldsymbol{W}_2$ produces a better solution. The performance degradation in this procedure is negligible since the solution is insensitive to the weighting matrix.

4 Feasibility of two-stage solution

The SDR problem is equivalent to its CWLS form if the SDR solution is rank-one and the SDR solution is feasible. In this section, we perform the feasibility study by applying the rank analysis. The stage-one SDR solution is rank-one at the small noise levels when $\boldsymbol{G}_1$ is full column rank, i.e.,

$$\operatorname{rank}(\boldsymbol{G}_1) = 2(q+K)M. \tag{41}$$

4.1 Rank of $\boldsymbol{G}_1$

In order to fulfill $\boldsymbol{G}_1$ to be full column rank, the number of rows in $\boldsymbol{G}_1$ should be greater than that of the columns, yielding

$$K \geqslant \frac{2q}{N-2}. \tag{42}$$

The column rank is determined by the maximum number of linearly independent columns in $\boldsymbol{G}_1$. Let the p-th column of $\boldsymbol{G}_1$ be $\boldsymbol{g}_1^{(p)}$, and the rank of $\boldsymbol{G}_1$ be P. As a result, there are P linearly independent columns in $\boldsymbol{G}_1$. Thus, the equation

$$\sum_{p=1}^{P} c_p \boldsymbol{g}_1^{(p)} = \boldsymbol{0}, \tag{43}$$

can only be satisfied by having

$$c_1 = c_2 = \cdots = c_P = 0. \tag{44}$$

From (42), N needs to be greater than or equal to 3. Assuming sufficient K, we provide a detailed analysis for the rank of $\boldsymbol{G}_1$ by considering varying (M, N) starting from their smallest value $(1, 3)$. In the following, we first consider the 3-D case ($q = 3$), and the rank analysis for the 2-D case ($q = 3$) is provided in Appendix B.

(1) ($M = 1$, $N = 3$). The positions of three sensors are $\boldsymbol{s}_1$, $\boldsymbol{s}_2$, and $\boldsymbol{s}_3$, and the size of $\boldsymbol{G}_1$ is $3K \times (2K+6)$. Let us define the vector by $\boldsymbol{c} = [c_1, c_2, \ldots, c_P]^{\mathrm{T}}$. Obviously, the length of vector $\boldsymbol{c}$ is $3K$. The first three columns of $\boldsymbol{G}_1$ give

$$\sum_{k=1}^{K} c_{3k-2}\boldsymbol{s}_1 + \sum_{k=1}^{K} c_{3k-1}\boldsymbol{s}_2 + \sum_{k=1}^{K} c_{3k}\boldsymbol{s}_3 = \boldsymbol{0}. \tag{45}$$

If the positions of $\boldsymbol{s}_1$, $\boldsymbol{s}_2$, and $\boldsymbol{s}_3$ are not coplanar, Eq. (45) implies

$$\sum_{k=1}^{K} c_{3k-2} = \sum_{k=1}^{K} c_{3k-1} = \sum_{k=1}^{K} c_{3k} = 0. \tag{46}$$

Applying the 4th to the 6th columns to (43) yields

$$\sum_{k=1}^{K} k c_{3k-2} = \sum_{k=1}^{K} k c_{3k-1} = \sum_{k=1}^{K} k c_{3k} = 0. \tag{47}$$

The subsequent K columns of $\boldsymbol{G}_1$ give

$$\sum_{i=1}^{3} c_{3k-3+i} d_{3k-3+i} = 0,\ k = 1, 2, \ldots, K. \tag{48}$$

Applying the last K columns produces

$$\sum_{i=1}^{3} c_{3k-3+i} = 0,\ k = 1, 2, \ldots, K. \tag{49}$$

There are $2K+6$ equations for (46)–(49). Unfortunately, they are not independent, and two correlated equations can be found. The sum of all terms on the left sides of (46) is equal to the sum of all K terms of (49). Hence, two sets of equations (46) and (49) are linearly dependent. Besides, the sum of the left terms in (47) is equal to the sum of k times (49). As a result, the column rank of $\boldsymbol{G}_1$ is $2K+4$ for the sufficient K.

(2) ($M=1$, $N=4$). The positions of four antennas are $\boldsymbol{s}_1$, $\boldsymbol{s}_2$, $\boldsymbol{s}_3$, and $\boldsymbol{s}_4$, and the size of $\boldsymbol{G}_1$ is $4K\times(2K+6)$. If $\boldsymbol{s}_1$, $\boldsymbol{s}_2$, and $\boldsymbol{s}_3$ are not parallel to one another, they span the 3-D space. Thus, $\boldsymbol{s}_4$ can be expressed as

$$\boldsymbol{s}_4=[\boldsymbol{s}_1,\boldsymbol{s}_2,\boldsymbol{s}_3][\lambda_1,\lambda_2,\lambda_3]^{\mathrm{T}}, \tag{50}$$

where λ_1, λ_2, λ_3 are not equal to zero.

As a result, the first three columns of $\boldsymbol{G}_1$ give

$$\sum_{i=1}^{4}\sum_{k=1}^{K}c_{4k-4+i}\boldsymbol{s}_i=\boldsymbol{0}. \tag{51}$$

Substituting (50) into (51) yields

$$\sum_{i=1}^{3}\sum_{k=1}^{K}(c_{4k-4+i}+\lambda_i c_{4k})\boldsymbol{s}_i=\boldsymbol{0}. \tag{52}$$

Therefore, we have

$$\sum_{k=1}^{K}(c_{4k-4+i}+\lambda_i c_{4k})=0,\ i=1,2,3. \tag{53}$$

Similarly, applying the 4th to 6th columns to (43) produces

$$\sum_{k=1}^{K}k(c_{4k-4+i}+\lambda_i c_{4k})=0,\ i=1,2,3. \tag{54}$$

Correspondingly, Eq. (47) becomes

$$\sum_{i=1}^{4}c_{4k-4+i}d_{4k-4+i}=0,\ k=1,2,\ldots,K. \tag{55}$$

The last K columns give

$$\sum_{i=1}^{4}c_{4k-4+i}=0,\ k=1,2,\ldots,K. \tag{56}$$

The number of equations (53)–(56) is $2K+6$, and they are linearly independent. Hence, there are totally $2K+6$ independent equations, indicating $\mathrm{rank}(\boldsymbol{G}_1)=2K+6$ for the sufficient $K\geqslant 3$, obtained by (42).

(3) ($M\geqslant 2$, $N=3$). The size of $\boldsymbol{G}_1$ is $3KM\times 2(K+3)M$, and the length of vector $\boldsymbol{c}$ is $3KM$. Although the number of the equations (46)–(49) are increased to $2(K+3)M$, $2M$ sets of equations are linearly dependent. Therefore, the rank of $\boldsymbol{G}_1$ is $2(K+2)M$ and never to be full column rank for the sufficient K.

(4) ($M\geqslant 2$, $N\geqslant 4$). Although the size of $\boldsymbol{G}_1$ is increased to $KMN\times 2(q+K)M$, $2(q+K)M$ sets of equations are still linearly independent due to the sufficient sensors of $N\geqslant 4$. As a result, $\boldsymbol{G}_1$ is always full column matrix.

The $\boldsymbol{G}_1$ is full column matrix for $N\geqslant 4$ regardless of the value of M. Thus, the stage-one SDR solution is rank-one and feasible to provide an estimated value for the unknown. Similar to the analysis for the rank of $\boldsymbol{G}_1$, we conduct the feasibility analysis for the stage-two SDR by applying the rank of $\boldsymbol{G}_2$.

4.2 Rank of $\boldsymbol{G}_2$

The size of $\boldsymbol{G}_2$ is $(2q+K)M \times (2qM+q+1)$. In order to satisfy $\text{rank}(\boldsymbol{G}_2) = 2qM+q+1$, the number of rows in $\boldsymbol{G}_2$ needs to be larger than or equal to that of the columns, producing $KM \geqslant 4$ for $q=3$. For the sufficient K, we derive the rank of $\boldsymbol{G}_2$ by considering varying M starting from one.

(1) $M=1$. The size of $\boldsymbol{G}_2$ is $(6+K)\times 10$. There is only one transceiver, and its starting position and velocity are $\boldsymbol{t}_{1,0}^o$ and $\boldsymbol{v}_1^o$, respectively. Besides, j is equal to k for $M=1$. Applying the first three columns of $\boldsymbol{G}_2$ yields

$$\sum_{k=1}^{K} c_{6+k}\boldsymbol{t}_{1,0} + \sum_{k=1}^{K} k c_{6+k}\boldsymbol{v}_1 = 0. \tag{57}$$

Considering $\boldsymbol{t}_{1,0}$ not parallel to $\boldsymbol{v}_1$, we arrive at

$$\sum_{k=1}^{K} c_{6+k} = 0, \quad \sum_{k=1}^{K} k c_{6+k} = 0. \tag{58}$$

By applying (58), the 4th–9th columns of $\boldsymbol{G}_2$ give

$$c_1 = c_2 = \cdots = c_6 = 0. \tag{59}$$

Finally, the last column of $\boldsymbol{G}_2$ gives

$$\sum_{k=1}^{K} c_{6+k} = 0. \tag{60}$$

Eqs. (58)–(60) are not linearly independent since the left equation of (58) is the same as (60). As a result, the maximum value of P can only be 8 to ensure Eq. (44) is the solution of (43). The rank of $\boldsymbol{G}_2$ is 8, which is less than the number of columns. Hence, the stage-two SDR is infeasible.

(2) $M=2$. The size of $\boldsymbol{G}_2$ increases to $(12+2K)\times 16$, and the starting positions and velocities of two transceivers are $\boldsymbol{t}_{1,0}^o$, $\boldsymbol{t}_{2,0}^o$, $\boldsymbol{v}_1^o$, and $\boldsymbol{v}_2^o$, respectively. Applying the last column of $\boldsymbol{G}_2$ yields

$$\sum_{k=1}^{K} c_{11+2k} = -\sum_{k=1}^{K} c_{12+2k}. \tag{61}$$

Substituting (1) and applying the first three columns to (43) give

$$\sum_{k=1}^{K} c_{11+2k}\boldsymbol{t}_{1,0} + \sum_{k=1}^{K} c_{12+2k}\boldsymbol{t}_{2,0} + \sum_{k=1}^{K} k c_{11+2k}\boldsymbol{v}_1 + \sum_{k=1}^{K} k c_{12+2k}\boldsymbol{v}_2 = 0. \tag{62}$$

Similar to (50), $\boldsymbol{t}_{2,0}$ is expressed by the form in term of $\boldsymbol{t}_{1,0}$, $\boldsymbol{v}_1$, and $\boldsymbol{v}_2$, yielding

$$\boldsymbol{t}_{2,0} = [\boldsymbol{t}_{1,0}, \boldsymbol{v}_1, \boldsymbol{v}_2][\gamma_1, \gamma_2, \gamma_3]^{\mathrm{T}}, \tag{63}$$

where γ_1, γ_2, γ_3 are not equal to zero. Provided that $\boldsymbol{t}_{1,0}$, $\boldsymbol{v}_1$, and $\boldsymbol{v}_2$ are not parallel to each other. Inserting (63) into (62) and applying (61) give

$$\sum_{k=1}^{K} c_{11+2k} = \sum_{k=1}^{K} k c_{12+2k} = \sum_{k=1}^{K} k c_{11+2k} = 0. \tag{64}$$

From the 4th–15th columns of $\boldsymbol{G}_2$, using (61) and (64), we arrive at

$$c_1 = c_2 = \cdots = c_{12} = 0. \tag{65}$$

Eqs. (61), (64), and (65) are linearly independent. Thus, the rank of $\boldsymbol{G}$ is 16, and $\boldsymbol{G}$ is full column rank. The stage-two SDR solution is rank-one and feasible.

(3) $M \geqslant 3$. Each transceiver contributes K rows to $\boldsymbol{G}_2$. Two transceivers are sufficient to guarantee $\boldsymbol{G}_2$ to be full column rank. Adding the new rows does not change the rank. As a result, the stage-two SDR solution is still rank-one, and the solution is feasible.

In summary, the minimum N is 4 for the stage-one SDR, and the minimum M is 2 for the stage-two SDR. Hence, the minimum value of (M, N) is (2, 4) for the two-stage SDR solution. In this situation, both SDR solutions tend to be rank-one, and the localization result is guaranteed to be reliable.

5 Performance analysis

In this section, the CRLB of this problem is derived. In addition, the performance of the two-stage SDR solutions is proven to approach CRLB accuracy sufficiently. For notation simplicity, we shall use the symbol $\boldsymbol{\nabla}_{\boldsymbol{a},\boldsymbol{b}}$ to denote the partial derivative, i.e., $\boldsymbol{\nabla}_{\boldsymbol{a},\boldsymbol{b}} = \frac{\partial \boldsymbol{a}}{\partial \boldsymbol{b}^{\mathrm{T}}}$.

5.1 CRLB derivation

For the proposed localization problem, the independent variables are $\boldsymbol{\varphi}^o = [\boldsymbol{u}^{o\mathrm{T}}, \boldsymbol{t}_0^{o\mathrm{T}}, \boldsymbol{v}^{o\mathrm{T}}]^{\mathrm{T}}$. According to the measurement equation, the fisher information matrix (FIM) is given by

$$\boldsymbol{F} = \boldsymbol{\nabla}_{\boldsymbol{d},\boldsymbol{\varphi}^o}^{\mathrm{T}} \boldsymbol{\Sigma}^{-1} \boldsymbol{\nabla}_{\boldsymbol{d},\boldsymbol{\varphi}^o}, \tag{66}$$

where $\boldsymbol{\nabla}_{\boldsymbol{d},\boldsymbol{\varphi}^o} \in \mathbb{R}^{KMN\times(q+2qM)}$ is defined as

$$[\boldsymbol{\nabla}_{\boldsymbol{d},\boldsymbol{\varphi}^o}]_{p,1:q} = \boldsymbol{\rho}_{\boldsymbol{u}^o,\boldsymbol{t}_j^o}^{\mathrm{T}}, \tag{67a}$$

$$[\boldsymbol{\nabla}_{\boldsymbol{d},\boldsymbol{\varphi}^o}]_{p,m_1+q+(1:q)} = \boldsymbol{\rho}_{\boldsymbol{t}_j^o,\boldsymbol{u}^o}^{\mathrm{T}} + \boldsymbol{\rho}_{\boldsymbol{t}_j^o,\boldsymbol{s}_i}^{\mathrm{T}}, \tag{67b}$$

$$[\boldsymbol{\nabla}_{\boldsymbol{d},\boldsymbol{\varphi}^o}]_{p,m_2+q+(1:q)} = k(\boldsymbol{\rho}_{\boldsymbol{t}_j^o,\boldsymbol{u}^o} + \boldsymbol{\rho}_{\boldsymbol{t}_j^o,\boldsymbol{s}_i})^{\mathrm{T}}, \tag{67c}$$

where $m_1 = q(m-1)$, $m_2 = q(m+M-1)$, $p = (j-1)N + i$, $j = (k-1)M + m$, $m = 1, 2, \ldots, M$, $k = 1, \ldots, K$.

As a result, the CRLB of this problem is

$$\mathrm{CRLB}(\boldsymbol{\varphi}^o) = \boldsymbol{F}^{-1} = (\boldsymbol{\nabla}_{\boldsymbol{d},\boldsymbol{\varphi}^o}^{\mathrm{T}} \boldsymbol{\Sigma}^{-1} \boldsymbol{\nabla}_{\boldsymbol{d},\boldsymbol{\varphi}^o})^{-1}. \tag{68}$$

5.2 Performance of two-stage

The CWLS problem (12) is equivalent to the stage-one SDR problem (19) when its solution is rank-one. Thus, the estimation error of the stage-one SDR solution is expressed by (24), and its covariance is approximated by (25). Similar to the stage-one SDR, the stage-two SDR solution is also a solution to the CWLS problem (35) if the SDR solution is rank-one. As s result, the covariance of the estimation error in the stage-two SDR solution is obtained by (38).

Inserting (25) into (31) produces $\boldsymbol{W}_2$, which is then applied to (38). As a result, the covariance of the estimation error $\Delta\boldsymbol{\varphi}$ is also given by

$$\mathrm{cov}(\Delta\boldsymbol{\varphi}) \simeq (\boldsymbol{K}^{\mathrm{T}} \boldsymbol{\Sigma}^{-1} \boldsymbol{K})^{-1}, \tag{69}$$

where $\boldsymbol{K} = \boldsymbol{B}_1^{-1} \boldsymbol{A}_1 \boldsymbol{B}_2^{-1} \boldsymbol{A}_2$. The form of expression (69) is similar to that of (68). Obviously, the covariance can approach the CRLB if satisfying $\boldsymbol{K} \simeq \boldsymbol{\nabla}_{\boldsymbol{d},\boldsymbol{\varphi}^o}$. In Appendix C, we provide a detailed proof for $\boldsymbol{K} \simeq \boldsymbol{\nabla}_{\boldsymbol{d},\boldsymbol{\varphi}^o}$. Therefore, the MSE of the estimation error $\boldsymbol{\varphi}$ is able to approach its CRLB.

5.3 Closed-form solution

Similar to the two-stage SDR, the closed-form solution also avails the pseudo-linear equation (7). Thus, the estimate of $\boldsymbol{y}_1$ is obtained by applying the WLS method. Unfortunately, the constrained relationships among the variables in $\boldsymbol{y}_1$ are not considered, and the stage-one WLS solution performs poorly. A feasible method to improve the performance is to apply the multi-stage WLS solution. Similar to the stage-two SDR solution, the variable $\boldsymbol{y}_2$ is defined, and the stage-two WLS solution is proposed by exploiting the constrained relationships among the variables. In the stage-two WLS, the constrained relationship between $\boldsymbol{u}^o$ and $\boldsymbol{u}^{o\mathrm{T}}\boldsymbol{u}^o$ fails to be established. Hence, the solution of the stage-two WLS needs to be further refined by designing the stage-three WLS. In the following, we call it a multi-stage WLS for a clear description. As a result, the multi-stage WLS solution performs well enough.

6 Evaluation

In this section, the performance of the two-stage SDR solution is examined by simulations. The positions of sensors used in the simulations are randomly generated according to uniform distribution $[-100, 100]$ m.

Table 1 Positions of eight sensors in 2-D simulations (m)

ID	1	2	3	4	5	6	7	8
x	-60	82	-10	39	59	5	-65	-46
y	89	67	15	24	91	76	96	-49

Table 2 Positions of nine sensors in 3-D simulations (m)

ID	1	2	3	4	5	6	7	8	9
x	-21	-58	34	-70	76	-70	65	50	-96
y	65	-36	14	-5	54	58	75	33	95
z	35	-73	-66	82	-59	55	-95	1	-70

Table 3 Positions of eight transceivers in 2-D simulations (m)

ID	1	2	3	4	5	6	7	8
x	135	145	51	132	72	102	121	95
y	126	106	110	148	120	143	73	67

Table 4 Positions of eight transceivers in 3-D simulations (m)

ID	1	2	3	4	5	6	7	8
x	81	63	51	134	87	95	143	77
y	93	123	65	135	91	124	73	82
z	50	132	72	73	87	55	82	142

Owing to the high complexity of the SDP calculation, one of the random geometry configurations is used for performance evaluation, and they are listed in Table 1 for the 2-D and Table 2 for the 3-D case. The object position is set at $(300, 300)$ m for the 2-D and $(300, 300, 300)$ m for the 3-D case. To determine the object position, the transceivers are moving at the region near the object position, and their velocities are generated randomly according to the uniform distribution $[-1, 1]$ m/s. The starting positions of 9 mobile transceivers are also randomly produced from the uniform distribution $[50, 150]$ m, and one of the random geometry configurations is used for evaluation and listed in Table 3 for the 2-D and Table 4 for the 3-D case. The noise covariance is given by $\boldsymbol{\Sigma} = \sigma^2 \boldsymbol{I}$. The performance is evaluated using root mean square error (RMSE), defined as

$$\mathrm{RMSE}(\boldsymbol{u}) = \sqrt{\frac{1}{L}\sum_{l=1}^{L} \|\boldsymbol{u}^l - \boldsymbol{u}^o\|^2}, \tag{70a}$$

$$\mathrm{RMSE}(\boldsymbol{t}_0) = \frac{1}{M}\sqrt{\frac{1}{L}\sum_{l=1}^{L} \|\boldsymbol{t}_0^l - \boldsymbol{t}_0^o\|^2}, \tag{70b}$$

$$\mathrm{RMSE}(\boldsymbol{v}) = \frac{1}{M}\sqrt{\frac{1}{L}\sum_{l=1}^{L} \|\boldsymbol{v}^l - \boldsymbol{v}^o\|^2}, \tag{70c}$$

where $\boldsymbol{u}^l$, $\boldsymbol{t}_0^l$, and $\boldsymbol{v}^l$ are the estimates in the l-th ensemble run. L is the number of Monte Carlo (MC) runs and L is adopted as 1000 in the simulations. The simulations are conducted by MATLAB, in which the SDP solver is SeDuMi. For performance comparison, we also develop the two-stage WLS (TSWLS) and the multi-stage WLS (MSWLS) solutions, which are described in Subsection 5.2. In addition, we also designed the relaxed SDP (RSDP) solution [43], which is also included as a performance comparison.

6.1 Performance with varying noise level σ

We first examine the performance with varying noise level σ for two different cases.

Scenario 1. The performance of the 2-D case is examined. M and N are kept at 3 and 4, respectively, and K is set at 10. The position parameters are the same as those of the first three transceivers in Table 3 and the first four sensors in Table 1. The RMSE performance of object position estimation is shown in Figure 2(a). Since the constrained relationships among the variables are not fully considered,

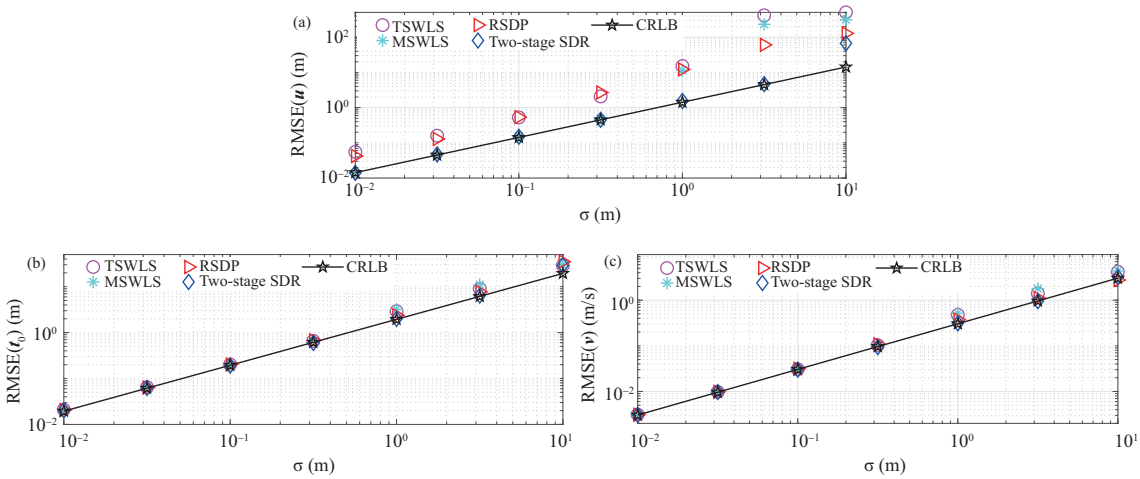

Figure 2 (Color online) Performance of 2-D case with varying σ when using $M = 3$ mobile transceivers, $N = 4$ sensors, $K = 10$ time steps. RMSE comparison for (a) object position estimation, (b) starting position estimation, and (c) velocity estimation.

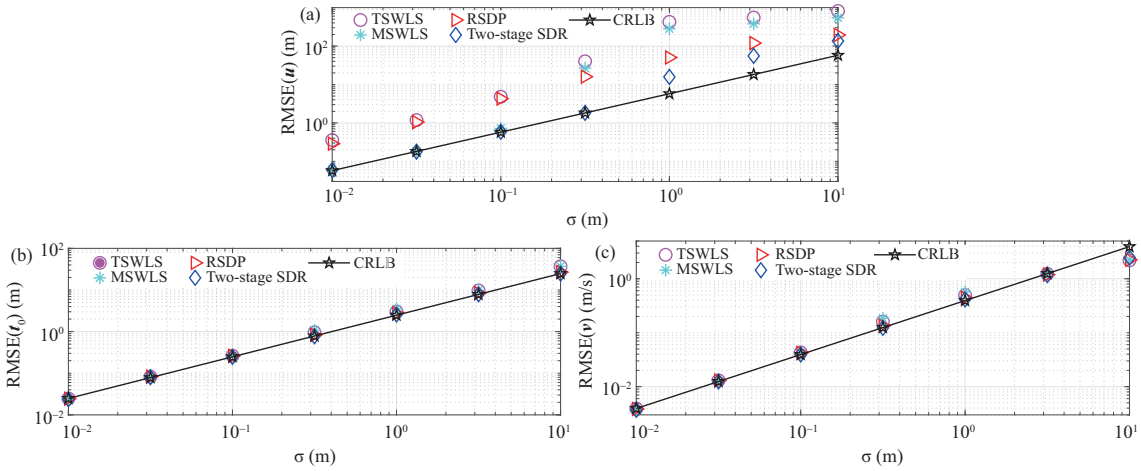

Figure 3 (Color online) Performance of 3-D case with varying σ when using $M = 3$ mobile transceivers, $N = 5$ sensors, $K = 10$ time steps. RMSE comparison for (a) object position estimation, (b) starting position estimation, and (c) velocity estimation.

the TSWLS and RSDP solutions perform poorly at the entire noise levels tested. The RMSE of the MSWLS approaches its CRLB at low noise levels, whereas it deviates from its CRLB at $\sigma \geqslant 1.0$ m. In contrast, the RMSE curve of the two-stage SDR is closer to the CRLB than that of the MSWLS, especially at the high noise levels of 1.0 m $\leqslant \sigma \leqslant$ 3.1 m.

Figures 2(b) and (c) show the RMSE performance in the estimation of starting positions and velocities, respectively. The two-stage SDR solution only refines the estimate of object position by availing of the constraint (34) and has no impact on the performance of the starting position and velocity estimation. Hence, the performance of the two-stage SDR in the estimation of starting positions and velocities is the same as that of the stage-one SDR. In addition, the RMSE curve of the MSWLS also almost overlaps with that of the TSWLS due to the same reason.

Scenario 2. The performance of the 3-D case is examined with varying noise levels. M and N are kept at 3 and 5, respectively, and K is also set at 10. The position parameters are the same as those of the first three transceivers in Table 4 and the first five sensors in Table 2. The RMSE performance of object position estimation is shown in Figure 3(a). Most of the observations are almost similar to those of the 2-D case. The difference is that the RMSE of the TSWLS deviates from its CRLB at $\sigma \geqslant 0.1$ m, which is earlier than that of the 2-D case. In contrast, the two-stage SDR performs better, especially at high noise levels.

The starting positions and velocities of the mobile transceivers are estimated together with the object position. Figures 3(b) and (c) show their RMSEs as σ increases. Except for the high noise level of $\sigma = 10.0$ m, all the solutions provide almost comparable CRLB accuracy. Hence, the performance for

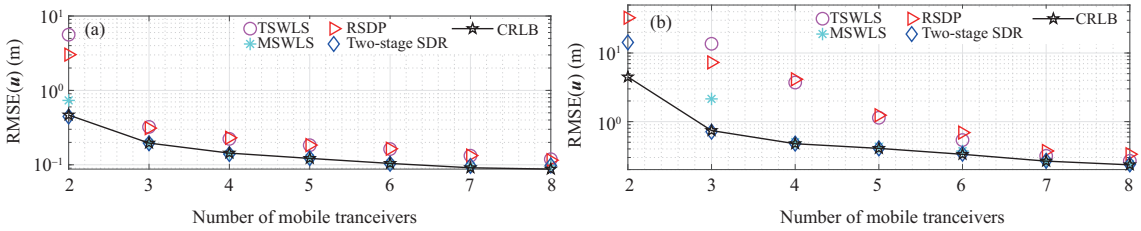

Figure 4 (Color online) Performance with varying M, when (a) using $\sigma = 0.1$ m, $N = 4$ sensors, and $K = 10$ time steps, for 2-D case, (b) using $\sigma = 0.1$ m, $N = 5$ sensors, and $K = 10$ time steps, for 3-D case.

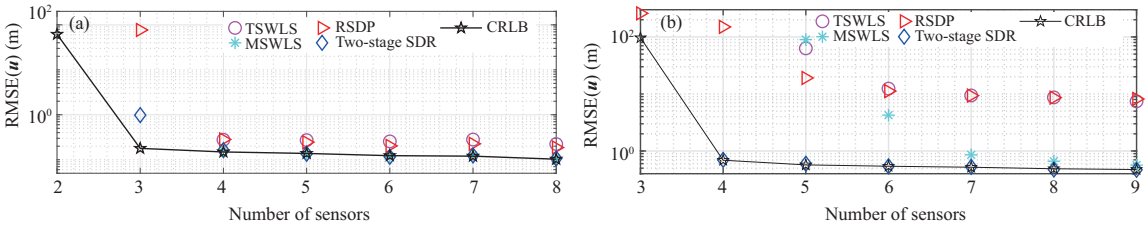

Figure 5 (Color online) Performance with varying N when using $\sigma = 0.1$ m, $M = 3$ mobile transceivers, and $K = 10$ time steps, for (a) 2-D case and (b) 3-D case.

the estimation of the starting positions and velocities is not evaluated in the following.

6.2 Performance with varying M

In this subsection, we investigate the performance with varying M, the number of mobile transceivers.

Scenario 3. The performance of the 2-D case is examined. N is set to be 4, and four sensor positions are the same as those of scenario 1. M is varied from 2 to 8, and the positions of M mobile transceivers are the same as those of Table 2. σ is kept at 0.1 m, and K is set at 10. Figure 4(a) shows the RMSE performance for the object position estimation. As shown in Figure 4(a), the RMSE performance of the two-stage SDR approaches its CRLB even if there are only two mobile transceivers. The two-stage SDR provides comparable CRLB accuracy when M is increased from 2 to 8. Although the MSTLS performs well at $N \geqslant 3$, its performance has a small gap with the CRLB at $N = 2$.

Scenario 4. The performance of the 3-D case is investigated. N is set to 5, and the five sensor positions are the same as those of scenario 2. M is also varied from 2 to 8, and the positions of M mobile transceivers are the same as those of Table 4. σ is also kept at 0.1 m, and K is also set at 10. Figure 4(b) shows the RMSE performance for the object position estimation. The closed-form solutions perform poorly, especially at a small number of mobile transceivers. For $M = 2$, the MSWLS fails to provide a solution for the object position estimation. In contrast, the two-stage SDR gives a solution for object position, although its performance is not close to the CRLB. When M is increased to 3, the performance of the two-stage SDR can attain the CRLB.

6.3 Performance with varying N

The minimum N is 3 for the 2-D case and 4 for the 3-case. In this subsection, we also investigate the performance with varying N, the number of sensors.

Scenario 5. The performance of the 2-D case is examined with varying N. σ is kept at 0.1 m, and K is set at 10. M is kept at 3, and the positions of three mobile transceivers are the same as those of scenario 1. In addition, we apply the first N sensors in Table 1 by considering varying N. The RMSE performance in the estimation of object estimation is plotted in Figure 5(a). For $N = 2$, the RMSEs of these solutions exceed the scope of the figure size and are not shown. The two-stage SDR can provide a solution for the object position at $N = 3$, which is consistent with the result in Section 5. When N is increased to 4, the RMSE of the MSWLS can approach the CRLB sufficiently.

Scenario 6. The performance of the 3-D case is examined. σ and K are set at 0.1 m and 10, respectively. M is also kept at 3, and the positions of three mobile transceivers are the same as those of scenario 2. Similarly, we apply N varying sensors in Table 2. Figure 5(b) shows the RMSE performance of the 3-D case. For the varying range of $4 \leqslant N \leqslant 9$, the two-stage SDR always provides comparable CRLB accuracy

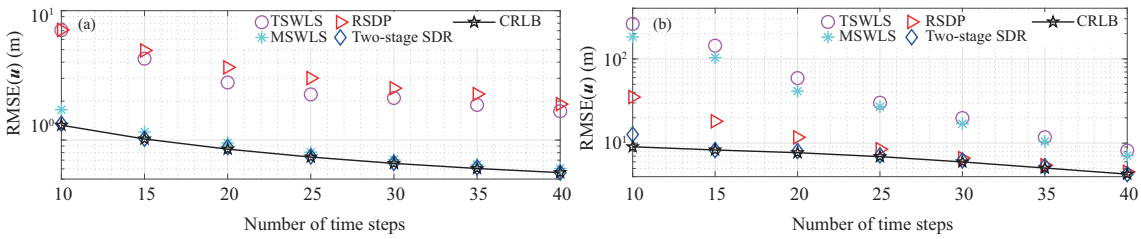

Figure 6 (Color online) Performance with varying K when (a) using $\sigma = 1.0$ m, $M = 3$ mobile transceivers, and $N = 4$ sensors, for 2-D case and (b) using $\sigma = 1.0$ m, $M = 3$ mobile transceivers, and $N = 5$ sensors, for 3-D case.

for its full exploitation of the constrained relationships. Unfortunately, the RSDP performs poorly due to its relaxed SDP form. The performance of the MSWLS is also poor except for $N \geqslant 7$.

6.4 Performance with varying time steps

Scenario 7. The performance of the 2-D case is examined with varying K. The parameter setup of sensors and mobile transceivers is the same as that of scenario 1. The noise level σ is kept at 1.0 m, and K is varied from 10 to 40 with an interval of 5. Figure 6(a) shows the RMSE performance in the object position estimation. As shown in Figure 6(a), the performance becomes better as K increases. The two-stage SDR performs well enough at the entire varying range of K. However, the RMSE of the TSWLS has a small gap with the CRLB for $K \leqslant 20$, confirming the disadvantage of the closed-form solution.

Scenario 8. The performance of the 3-D case is examined. The parameter setup of sensors and mobile transceivers is the same as that of scenario 2. The noise level σ is also kept at 1.0 m. Figure 6(b) shows the RMSE performance as K varies. Different from the 2-D case, the performance of the MSWLS has a large gap with the CRLB when K is varied from 10 to 40. The observations indicate that the closed-form solution of the 3-D case performs worse than that of the 2-D case due to the increasing of unknown parameters. In addition, the two-stage SDR solution performs best among these solutions, and its performance always approaches the CRLB except for $K = 10$.

7 Conclusion and future work

The mobile transceivers are used to address the blind area problem of object localization. Considering the motion parameters of the transceivers to be unavailable, we propose an explainable-AI-based two-stage solution for this localization problem. The feasibility of the two-stage solution is derived, and we require at least $(M = 2, N = 3)$ for the 2-D case and $(M = 2, N = 4)$ for the 3-D.

The relationships among the variables are difficult to include in the stage-one process, and the performance of the one-stage is poor. Hence, the explainable-AI-based two-stage solution is proposed to fully exploit the constrained relationships, and its performance is proven to approach the optimal accuracy sufficiently. Compared with the multi-stage closed-form solution, the explainable-AI-based two-stage solution performs better, especially at a small number of sensors and mobile transceivers, or in the presence of high noise levels. The proposed explainable-AI-based two-stage solution can be extended to many range-based localization problems where the object position is implicit in the constraints.

In real-world scenarios, for less open terrain, the transceiver needs to avoid obstacles. When K is large, it may not be possible to ensure that the transceiver is always in uniform linear motion. In future work, we will investigate the nonlinear motion of transceivers. There are many application scenarios for transceiver-based localization methods, such as sensor networks that mix fixed and dynamic sensors, underwater localization of AUVs, etc. In future research, the localization solution will be applied to a wider range of scenarios.

Acknowledgements This work was supported by National Natural Science Foundation of China (Grant No. 52102400), Zhejiang Provincial Natural Science Foundation of China (Grant No. LQ23F020001), Quzhou City Science and Technology Project (Grant Nos. 2023K252, 2023K248), Zhejiang Key R&D Plan (Grant No. 2017C03047), and Zhejiang Province Key Laboratory of Smart Management and Application of Modern Agricultural Resources (Grant No. 2020E10017).

References

1 Wu X, Qi H. Motion parameter estimation for mobile sources using semidefinite programming. IEEE Trans Mobile Comput, 2023, 22: 1066–1080
2 Fang K, Wang T, Zhou X, et al. A TOPSIS-based relocalization algorithm in wireless sensor networks. IEEE Trans Ind Inf, 2022, 18: 1322–1332
3 Wu X, Liu Y, Zhu X, et al. Efficient solutions for MIMO radar localization under unknown transmitter positions and offsets. IEEE Trans Wireless Commun, 2022, 21: 505–518
4 Wu X, Mao X, Qi H. Semidefinite relaxation for moving target localization in asynchronous MIMO systems. IEEE Trans Commun, 2024, 72: 1075–1089
5 Zhang C Z, Guo J, Yang C Y. When the gain of predictive resource allocation for content delivery is large? Sci China Inf Sci, 2023, 66: 222302
6 Dehghani M, Aghababaiyan K. FOMP algorithm for direction of arrival estimation. Phys Commun, 2018, 26: 170–174
7 Aghababaiyan K, Zefreh R G, Shah-Mansouri V. 3D-OMP and 3D-FOMP algorithms for DOA estimation. Phys Commun, 2018, 31: 87–95
8 Sun Y, Xie J, Han C, et al. Array element selection strategies for interference suppression in reconfigurable tripole antenna array systems. IEEE Trans Veh Technol, 2023, 72: 557–572
9 Moerman A, van Kerrebrouck J, Caytan O, et al. Beyond 5G without obstacles: mmWave-over-fiber distributed antenna systems. IEEE Commun Mag, 2022, 60: 27–33
10 Yuan W, Wu N, Guo Q, et al. TOA-based passive localization constructed over factor graphs: a unified framework. IEEE Trans Commun, 2019, 67: 6952–6965
11 Wang T, Xiong H, Ding H, et al. TDOA-based joint synchronization and localization algorithm for asynchronous wireless sensor networks. IEEE Trans Commun, 2020, 68: 3107–3124
12 Wang Y, Ho K C. An asymptotically efficient estimator in closed-form for 3-D AOA localization using a sensor network. IEEE Trans Wireless Commun, 2015, 14: 6524–6535
13 Sun Y, Ho K C, Wan Q. Eigenspace solution for AOA localization in modified polar representation. IEEE Trans Signal Process, 2020, 68: 2256–2271
14 Wang Z, Zhang H, Lu T, et al. Cooperative RSS-based localization in wireless sensor networks using relative error estimation and semidefinite programming. IEEE Trans Veh Technol, 2019, 68: 483–497
15 Wu X, Zhu X, Wang S, et al. Cooperative motion parameter estimation using RSS measurements in robotic sensor networks. J Network Comput Appl, 2019, 136: 57–70
16 Sun B, Guo Y, Li N, et al. Multiple target counting and localization using variational Bayesian EM algorithm in wireless sensor networks. IEEE Trans Commun, 2017, 65: 2985–2998
17 Nguyen T V, Jeong Y, Shin H, et al. Least square cooperative localization. IEEE Trans Veh Technol, 2015, 64: 1318–1330
18 Mukhopadhyay B, Srirangarajan S, Kar S. Signal strength-based cooperative sensor network localization using convex relaxation. IEEE Wireless Commun Lett, 2020, 9: 2207–2211
19 Zhu G X, Lyu Z H, Jiao X, et al. Pushing AI to wireless network edge: an overview on integrated sensing, communication, and computation towards 6G. Sci China Inf Sci, 2023, 66: 130301
20 Zhang S, Staudinger E, Jost T, et al. Distributed direct localization suitable for dense networks. IEEE Trans Aerosp Electron Syst, 2020, 56: 1209–1227
21 Yu Z, Li J, Guo Q, et al. Efficient direct target localization for distributed MIMO radar with expectation propagation and belief propagation. IEEE Trans Signal Process, 2021, 69: 4055–4068
22 Sun Y, Ho K C, Wan Q. Solution and analysis of TDOA localization of a near or distant source in closed form. IEEE Trans Signal Process, 2019, 67: 320–335
23 Kazemi S A R, Amiri R, Behnia F. Efficient closed-form solution for 3-D hybrid localization in multistatic radars. IEEE Trans Aerosp Electron Syst, 2021, 57: 3886–3895
24 Wang G, Ho K C. Convex relaxation methods for unified near-field and far-field TDOA-based localization. IEEE Trans Wireless Commun, 2019, 18: 2346–2360
25 Wu X, Qi H, Xiong N. Rank-one semidefinite programming solutions for mobile source localization in sensor networks. IEEE Trans Netw Sci Eng, 2021, 8: 638–650
26 Zheng R, Wang G, Ho K C. Accurate semidefinite relaxation method for elliptic localization with unknown transmitter position. IEEE Trans Wireless Commun, 2021, 20: 2746–2760
27 Sheng M, Zhou D, Bai W G, et al. Coverage enhancement for 6G satellite-terrestrial integrated networks: performance metrics, constellation configuration and resource allocation. Sci China Inf Sci, 2023, 66: 130303
28 Shao H-J, Zhang X-P, Wang Z. Efficient closed-form algorithms for AOA based self-localization of sensor nodes using auxiliary variables. IEEE Trans Signal Process, 2014, 62: 2580–2594
29 Amiri R, Behnia F. An efficient weighted least squares estimator for elliptic localization in distributed MIMO radars. IEEE Signal Process Lett, 2017, 24: 902–906
30 Noroozi A, Sebt M A, Oveis A H. Efficient weighted least squares estimator for moving target localization in distributed MIMO radar with location uncertainties. IEEE Syst J, 2019, 13: 4454–4463
31 Song H, Wen G, Zhu L, et al. A novel TSWLS method for moving target localization in distributed MIMO radar systems. IEEE Commun Lett, 2019, 23: 2210–2214
32 Park C H, Chang J H. Closed-form localization for distributed MIMO radar systems using time delay measurements. IEEE Trans Wireless Commun, 2016, 15: 1480–1490
33 Nocedal J, Wright S J. Numerical Optimization. 2nd ed. New York: Springer, 2006
34 Qi H, Mo L, Wu X. SDP relaxation methods for RSS/AOA-based localization in sensor networks. IEEE Access, 2020, 8: 55113–55124
35 Wu X, Lin Q, Qi H. Cooperative multiple rigid body localization via semidefinite relaxation using range measurements. IEEE Trans Signal Process, 2022, 70: 4788–4803
36 Sadeghi M, Behnia F, Amiri R. Optimal geometry analysis for elliptic localization in multistatic radars with two transmitters. IEEE Trans Aerosp Electron Syst, 2022, 58: 697–703
37 Qi H, Wu X, Jia L. Semidefinite programming for unified TDOA-based localization under unknown propagation speed. IEEE Commun Lett, 2020, 24: 1971–1975
38 Xing C, Zhao X, Xu W, et al. A framework on hybrid MIMO transceiver design based on matrix-monotonic optimization. IEEE Trans Signal Process, 2019, 67: 3531–3546

39 Wu Q, Zhang R. Towards smart and reconfigurable environment: intelligent reflecting surface aided wireless network. IEEE Commun Mag, 2020, 58: 106–112
40 Wymeersch H, He J, Denis B, et al. Radio localization and mapping with reconfigurable intelligent surfaces: challenges, opportunities, and research directions. IEEE Veh Technol Mag, 2020, 15: 52–61
41 Liu Y, Wang Y, Wang J, et al. Distributed 3D relative localization of UAVs. IEEE Trans Veh Technol, 2020, 69: 11756–11770
42 Ho K C. Localization through transceivers in unknown constant velocity trajectories. IEEE Trans Signal Process, 2022, 70: 3011–3028
43 Wu X, Shen Y, Zhu X, et al. Semidefinite programming solutions for Elliptic localization in asynchronous radar networks. IEEE Trans Aerosp Electron Syst, 2022, 58: 3385–3398

Appendix A Definitions of $\boldsymbol{G_2}$, $\boldsymbol{B_2}$, and $\boldsymbol{h_2}$

Obviously, $\boldsymbol{G}_2 \in \mathbb{R}^{(2qM+KM)\times(q+2qM)}$, the nonzero elements of $\boldsymbol{G}_2$ are defined as

$$\begin{aligned}&[\boldsymbol{G}_2]_{m_1+(1:q),qm+(1:q)} = \boldsymbol{I},\ [\boldsymbol{G}_2]_{m_1+(1:q),q(m+M)+(1:q)} = \boldsymbol{I},\ [\boldsymbol{G}_2]_{M_1+j,1:q} = \boldsymbol{t}_j^{\mathrm{T}},\\ &[\boldsymbol{G}_2]_{M_1+j,q+1+qM} = -0.5,\ [\boldsymbol{G}_2]_{M_1+j,qm+(1:q)} = -0.5\boldsymbol{t}_j^{\mathrm{T}},\ [\boldsymbol{G}_2]_{M_1+j,q(m+M)+(1:q)} = -0.5k\boldsymbol{t}_j^{\mathrm{T}},\end{aligned} \tag{A1}$$

where $\boldsymbol{t}_j = [\boldsymbol{\phi}]_{m_1+(1:q)} + k[\boldsymbol{\phi}]_{m_2+(1:q)}$, $m_1 = q(m-1)$, $m_2 = q(m+M-1)$, $M_1 = 2qM$, $j = (k-1)M+m$, $m = 1, 2, \ldots, M$, $k = 1, \ldots, K$.

Besides, the vector $\boldsymbol{h}_2 \in \mathbb{R}^{2qM+KM}$ is defined as

$$\begin{aligned}&[\boldsymbol{h}_2]_{m_1+(1:q)} = [\boldsymbol{\phi}]_{m_1+(1:q)},\ [\boldsymbol{h}_2]_{m_2+(1:q)} = [\boldsymbol{\phi}]_{m_2+(1:q)},\\ &[\boldsymbol{h}_2]_{M_1+j} = 0.5(\boldsymbol{t}_j^{\mathrm{T}}\boldsymbol{t}_j - [\boldsymbol{\phi}]^2_{M_1+j}).\end{aligned} \tag{A2}$$

In addition, $\boldsymbol{B}_2 \in \mathbb{R}^{(2qM+KM)\times(2qM+KM)}$ is given by

$$\begin{aligned}&[\boldsymbol{B}_2]_{1:M_1,1:M_1} = -\boldsymbol{I},\ [\boldsymbol{B}_2]_{M_1+j,m_1+(1:q)} = (\boldsymbol{u}^o - 0.5\boldsymbol{t}_j)^{\mathrm{T}} \simeq (\boldsymbol{u} - 0.5\boldsymbol{t}_j)^{\mathrm{T}},\\ &[\boldsymbol{B}_2]_{M_1+j,m_2+(1:q)} = k(\boldsymbol{u}^o - 0.5\boldsymbol{t}_j)^{\mathrm{T}} \simeq k(\boldsymbol{u} - 0.5\boldsymbol{t}_j)^{\mathrm{T}},\ [\boldsymbol{B}_2]_{M_1+j,M_1+j} = \alpha_j = [\boldsymbol{\phi}]_{M_1+j}.\end{aligned} \tag{A3}$$

In (A2) and (A3), $M_2 = 2qM + KM$, and the definitions of j, m, k, m_1, m_2, and M_1 are the same as those of (A1).

Appendix B Rank of $\boldsymbol{G_1}$ and $\boldsymbol{G_2}$ for 2-D case

The rank analysis for the 2-D case is relatively simple due to the reduction of the dimension, and the procedure is similar to that of the 3-D case.

Appendix B.1 Rank of $\boldsymbol{G_1}$

Obviously, two sensors ($N = 2$) are insufficient for the inequity of (42). Hence, the rank analysis of $\boldsymbol{G}_1$ is conducted by varying (M, N) also starting from $(1, 3)$.

(1) $M = 1$, $N = 3$. The size of $\boldsymbol{G}_1$ is $3K \times (2K+4)$, and the length of vector $\boldsymbol{c}$ is also $3K$. The positions $\boldsymbol{s}_1$ and $\boldsymbol{s}_2$ span the 2-D plane, and $\boldsymbol{s}_3$ can be expressed by

$$\boldsymbol{s}_3 = [\boldsymbol{s}_1, \boldsymbol{s}_2][\omega_1, \omega_2]^{\mathrm{T}}. \tag{B1}$$

Equating the first two columns of (43) gives

$$\sum_{k=1}^{K} c_{3k-2}\boldsymbol{s}_1 + \sum_{k=1}^{K} c_{3k-1}\boldsymbol{s}_2 + \sum_{k=1}^{K} c_{3k}\boldsymbol{s}_3 = \boldsymbol{0}. \tag{B2}$$

Inserting (B1) into (B2) results in

$$\sum_{k=1}^{K}(c_{3k-2} + \omega_1 c_{3k})\boldsymbol{s}_1 + \sum_{k=1}^{K}(c_{3k-1} + \omega_2 c_{3k})\boldsymbol{s}_2 = \boldsymbol{0}. \tag{B3}$$

Therefore, we have

$$\sum_{k=1}^{K}(c_{3k-2} + \omega_1 c_{3k}) = \sum_{k=1}^{K}(c_{3k-1} + \omega_2 c_{3k}) = 0. \tag{B4}$$

Similarly, applying the 3rd–4th columns to (43) yields

$$\sum_{k=1}^{K} k(c_{3k-2} + \omega_1 c_{3k}) = \sum_{k=1}^{K} k(c_{3k-1} + \omega_2 c_{3k}) = 0. \tag{B5}$$

In addition, the subsequent K columns give

$$\sum_{i=1}^{3} c_{3k-3+i}d_{3k-3+i} = 0,\ k = 1, 2, \ldots, K. \tag{B6}$$

Equating the last K columns produces

$$\sum_{i=1}^{3} c_{3k-3+i} = 0,\ k = 1, 2, \ldots, K. \tag{B7}$$

As a result, the $2K + 4$ equations of (B4)–(B7) are linearly independent, and $\boldsymbol{G}_1$ is full column rank for the sufficient $K \geqslant 4$.

(2) $M \geqslant 2$, $N \geqslant 3$. The number of columns in $\boldsymbol{G}_1$ is $4M + 2KM$. Applying a similar method to (B1)–(B3), we can obtain $4M$ independent equations for $N \geqslant 3$. The last $2KM$ columns also give $2KM$ independent equations, and they are also linearly independent with the front $4M$ equations. Hence, the rank of $\boldsymbol{G}_1$ is also $4M + 2KM$ and equal to the number of columns. $\boldsymbol{G}_1$ is always full column rank for the sufficient K.

Appendix B.2 Rank of $\boldsymbol{G_2}$

The size of $\boldsymbol{G}_2$ is $(4M + KM) \times (4M + 3)$, and $KM \geqslant 3$ needs to be satisfied to ensure $\boldsymbol{G}_2$ is full column rank. Similarly, let us consider the case of $M = 1$.

(1) $M = 1$. The size of $\boldsymbol{G}_2$ is $(4 + K) \times 7$, and j is equal to k for $M = 1$. Similar to (57), applying the first two columns yields

$$\sum_{k=1}^{K} c_{4+k}\boldsymbol{t}_{1,0} + \sum_{k=1}^{K} kc_{4+k}\boldsymbol{v}_1 = 0. \tag{B8}$$

Provided that $\boldsymbol{t}_{1,0}$ is not parallel to $\boldsymbol{v}_1$, we have

$$\sum_{k=1}^{K} c_{4+k} = 0, \quad \sum_{k=1}^{K} kc_{4+k} = 0. \tag{B9}$$

Equating the 3rd–6th columns to (43) gives

$$c_1 = c_2 = \cdots = c_4 = 0. \tag{B10}$$

The last column of $\boldsymbol{G}_2$ gives

$$\sum_{k=1}^{K} c_{4+k} = 0. \tag{B11}$$

Obviously, the first expression of (B9) is also (B11). As a result, the rank of $\boldsymbol{G}_2$ is 7, which is less than the number of columns. Hence, the stage-two SDR is also infeasible for $M = 1$.

(2) $M = 2$. The size of $\boldsymbol{G}_2$ is $(8 + 2K) \times 11$. The starting positions and velocities of two transceivers are $\boldsymbol{t}_{1,0}^o$, $\boldsymbol{v}_1^o$, $\boldsymbol{t}_{2,0}^o$, and $\boldsymbol{v}_2^o$, respectively. $\boldsymbol{t}_{1,0}^o$ and $\boldsymbol{v}_1^o$ span the 2-D plane, and $\boldsymbol{t}_{2,0}^o$ and $\boldsymbol{v}_2^o$ can be represented as

$$\boldsymbol{t}_{2,0} = [\boldsymbol{t}_{1,0}, \boldsymbol{v}_1][\nu_1, \nu_2]^{\mathrm{T}}, \boldsymbol{v}_2 = [\boldsymbol{t}_{1,0}, \boldsymbol{v}_1][\mu_1, \mu_2]^{\mathrm{T}}. \tag{B12}$$

Equating the last column of $\boldsymbol{G}_2$ to (43) yields

$$\sum_{k=1}^{K} c_{7+2k} = -\sum_{k=1}^{K} c_{8+2k}. \tag{B13}$$

Assuming $\boldsymbol{t}_{1,0}$ not parallel to $\boldsymbol{v}_1$. Inserting (B12) into (62) and applying (B13) give

$$\sum_{k=1}^{K}(1 + k\nu_1 - k\mu_1)c_{7+2k} = \sum_{k=1}^{K}(1 + k\mu_2 - k\nu_2)c_{8+2k} = 0. \tag{B14}$$

From the 3rd–10th columns of $\boldsymbol{G}_2$, we can obtain 8 independent equations. As a result, these equations are linearly independent. Thus, the rank of $\boldsymbol{G}$ is 11, and $\boldsymbol{G}$ is full column rank. The stage-two SDR solution is feasible.

(3) $M \geqslant 3$. Similar to the 3-D case, $\boldsymbol{G}_2$ is still a full column matrix when adding the new rows. Two transceivers are sufficient to guarantee that the stage-two SDR solution is feasible.

For the 2-D case, the minimum N is 3 for the stage-one SDR, and the minimum M is also 2 for the stage-two SDR. Hence, the minimum value of (M, N) is (2, 3) for the two-stage SDR solution.

Appendix C Proof for $\boldsymbol{K \simeq \nabla_{d,\varphi^o}}$

Direct multiplication yields $\boldsymbol{B}_1^{-1}\boldsymbol{A}_1$, given by

$$[\boldsymbol{B}_1^{-1}\boldsymbol{A}_1]_{p,m_1+(1:q)} = \boldsymbol{\rho}_{\boldsymbol{s}_i,\boldsymbol{t}_j}^{\mathrm{T}},\ [\boldsymbol{B}_1^{-1}\boldsymbol{A}_1]_{p,m_2+(1:q)} = k\boldsymbol{\rho}_{\boldsymbol{s}_i,\boldsymbol{t}_j}^{\mathrm{T}},\ [\boldsymbol{B}_1^{-1}\boldsymbol{A}_1]_{p,2qM+j} = -1. \tag{C1}$$

Similarly, $\boldsymbol{B}_2^{-1}\boldsymbol{A}_2$ is defined as

$$[\boldsymbol{B}_2^{-1}\boldsymbol{A}_2]_{p,m_1+(1:q)} = \boldsymbol{\rho}_{\boldsymbol{s}_i,\boldsymbol{t}_j}^{\mathrm{T}},\ [\boldsymbol{B}_2^{-1}\boldsymbol{A}_2]_{p,m_2+(1:q)} = k\boldsymbol{\rho}_{\boldsymbol{s}_i,\boldsymbol{t}_j}^{\mathrm{T}},\ [\boldsymbol{B}_1^{-1}\boldsymbol{A}_1]_{p,2qM+j} = 1. \tag{C2}$$

From $\boldsymbol{A}_2 = \boldsymbol{G}_2\boldsymbol{H}_2$, $\boldsymbol{A}_2$ is also defined as

$$[\boldsymbol{A}_2]_{1:2qM,q+(1:2qM)} = \boldsymbol{I},\ [\boldsymbol{A}_2]_{2qM+j,1:q} = \boldsymbol{t}_j - \boldsymbol{u},$$

$$[\boldsymbol{A}_2]_{2qM+j,qm+(1:q)} = -0.5\boldsymbol{t}_j^{\mathrm{T}},\ [\boldsymbol{A}_2]_{2qM+j,q(m+M)+(1:q)} = -0.5k\boldsymbol{t}_j^{\mathrm{T}}. \tag{C3}$$

Applying the inverse formula of the block matrix, we arrive at

$$\begin{aligned}&[\boldsymbol{B}_2^{-1}]_{1:2qM,1:2qM} = -\boldsymbol{I},\ [\boldsymbol{B}_2^{-1}]_{2qM+j,q(m-1)+(1:q)} = (0.5\boldsymbol{t}_j - \boldsymbol{u})\alpha_j^{-1},\\ &[\boldsymbol{B}_2^{-1}]_{2qM+j,q(m+M-1)+(1:q)} = k(0.5\boldsymbol{t}_j - \boldsymbol{u})\alpha_j^{-1},\ [\boldsymbol{B}_2]_{2qM+j,2qM+j} = \alpha_j^{-1}.\end{aligned} \tag{C4}$$

Direct multiplication gives

$$\begin{aligned}&[\boldsymbol{B}_2^{-1}\boldsymbol{A}_2]_{1:2qM,q+(1:2qM)} = -\boldsymbol{I},\ [\boldsymbol{B}_2^{-1}\boldsymbol{A}_2]_{2qM+j,1:q} = \boldsymbol{\rho}_{\boldsymbol{t}_j,\boldsymbol{u}}^{\mathrm{T}},\\ &[\boldsymbol{B}_2^{-1}\boldsymbol{A}_2]_{2qM+j,qm+(1:q)} = \boldsymbol{\rho}_{\boldsymbol{u},\boldsymbol{t}_j}^{\mathrm{T}},\ [\boldsymbol{B}_2^{-1}\boldsymbol{A}_2]_{2qM+j,q(m+M)+(1:q)} = k\boldsymbol{\rho}_{\boldsymbol{u},\boldsymbol{t}_j}^{\mathrm{T}}.\end{aligned} \tag{C5}$$

As a result, $\boldsymbol{B}_1^{-1}\boldsymbol{A}_1$ multiplying by $\boldsymbol{B}_2^{-1}\boldsymbol{A}_2$ yields K, and K is approximately equal to $\boldsymbol{\nabla}_{\boldsymbol{d},\boldsymbol{\varphi}^o}$.